

Synthesis, structure, and catalytic properties of *ansa*-zirconocenes, $\text{Me}_2\text{Si}(\text{RInd})_2\text{ZrCl}_2$ ($\text{R} = 2\text{-}p\text{-}$ or $3\text{-}p\text{-tolyl}$)

Sung Cheol Yoon ^a, Je-Woo Park ^b, Hyun Sook Jung ^a, Hyunjoon Song ^a, Joon T. Park ^{a,*},
Seong Ihl Woo ^b

^a Department of Chemistry, Korea Advanced Institute of Science and Technology, Taejeon, 305-701, South Korea

^b Department of Chemical Engineering, Korea Advanced Institute of Science and Technology, Taejeon, 305-701, South Korea

Received 18 November 1997; received in revised form 16 January 1998

Abstract

ansa-Ligands, $\text{Me}_2\text{Si}(\text{RInd})_2$ [$\text{R} = 2\text{-}p$ (**1**) and $3\text{-}p\text{-tolyl}$ (**2**)], have been prepared as a mixture of *rac*- and *meso*-isomers in a ratio of 1:1 from the reactions of Me_2SiCl_2 with cyanocuprates of 1-*p*-tolylindene and 2-*p*-tolylindene in diethyl ether, respectively. Pure *rac*-isomers, **1r** and **2r**, have been isolated by fractional recrystallization of **1** and **2**. Thermal diastereomerization of **1** and **2** between *rac*- and *meso*-isomers has been studied by ¹H-NMR spectroscopy. These results imply that **1** and **2** undergo the diastereomerization process by migration of silicon moiety and hydrogen atom, respectively. *ansa*-Zirconocenes, $\text{Me}_2\text{Si}(\text{RInd})_2\text{ZrCl}_2$ [$\text{R} = 2\text{-}p$ (**3**) and $3\text{-}p\text{-tolyl}$ (**4**)], have been prepared from the reactions of the corresponding dilithiated ligands with ZrCl_4 in diethyl ether and hexane at -78°C . The molecular structure of *rac*-**3** has been determined by a single crystal X-ray diffraction study. Propylene polymerization has been studied using *rac*-**3** and *meso*-**4** in the presence of methylaluminoxane (MAO). Catalyst *rac*-**3** produces a highly isotactic polypropylene (PP) at 0°C by the enantiomorphic site control mechanism and *meso*-**4** affords a syndiotactic dominant PP having a rr triad of 49% at -30°C by the chain end control mechanism. © 1998 Elsevier Science S.A. All rights reserved.

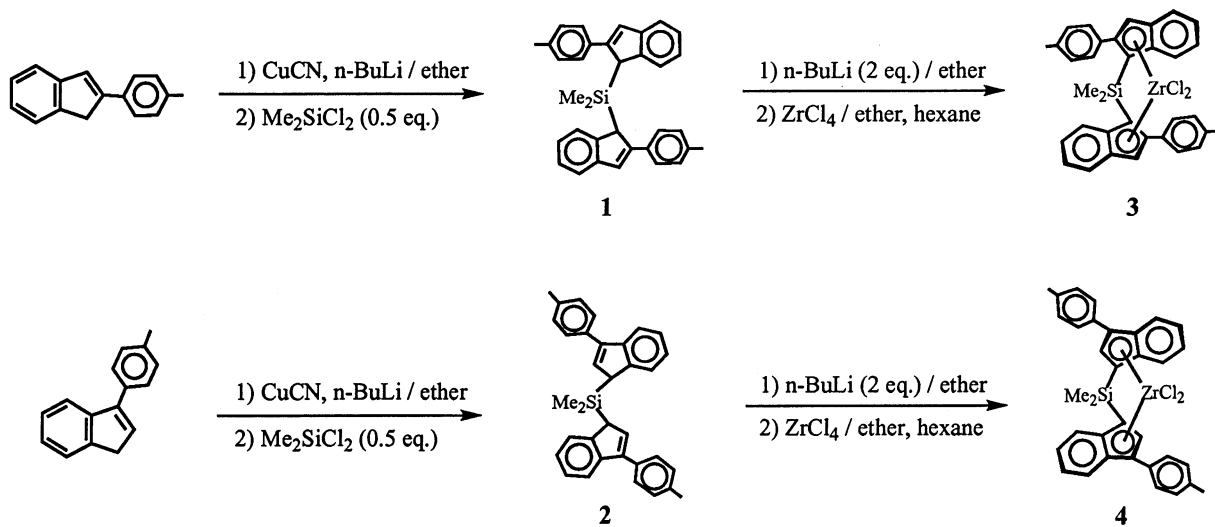
Keywords: *ansa*-Zirconocene; Tolyindene; Diastereomerization; Propylene polymerization; Crystal structure

1. Introduction

The development of homogeneous metallocene based catalysts for α -olefin polymerization has led to the tailored polymer synthesis with enhanced properties by a rational design of metallocene complexes. For example, C_2 -symmetric *ansa*-metallocene catalysts produce isotactic polypropylene (iPP) [1–4] and C_s -symmetric *ansa*-metallocene yield syndiotactic polypropylene (sPP) [5]. The bis(indenyl) ligand and its derivatives with proper substituents have been considerably employed as π -ligands of metallocenes. Unbridged mono-substituted indenyl complexes have shown their versatile catalytic properties caused by a rotation of

π -ligands during polymerization [6,7]. Waymouth and coworkers [7] have reported that unbridged $(2\text{-PhInd})_2\text{ZrCl}_2$ ($\text{Ph} = \text{C}_6\text{H}_5$) catalyst precursor polymerizes propylene to yield atactic-isotactic stereoblock polymers with elastomeric properties by a facile inter-conversion of the rotameric conformers of the catalyst. The introduction of a bridging group between the two π -ligands restricts the mobility of the π -ligands providing a rigid system which transfers the chirality information of the *ansa*-metallocene onto the growing polymer chain by the enantiomorphic site controlled process. Spaleck and coworkers [2] have reported that Me_2Si -bridged zirconocenes, $\text{Me}_2\text{Si}(\eta^5\text{-}2,4\text{-R}_2\text{Ind})_2\text{ZrCl}_2$ with 2-methyl and 4-aromatic groups substituted, are new optimized metallocene catalysts for isotactic propylene polymerization. The Me_2Si -bridge in *ansa*-metallocene

* Corresponding author. Fax: +82 42 8692810.



Scheme 1.

catalysts appears to be preferable over Me_2C - or two atom ethylene bridge, imposing high rigidity and favorable steric and electronic characteristics to *ansa*-metallocenes to produce high isotacticity and high molecular weight of polymers.

In previous work, we reported the synthesis of unbridged metallocene complexes, *rac*- and *meso*-(1-TolInd) $_2\text{ZrCl}_2$ (Tol = *p*- $\text{C}_6\text{H}_4\text{CH}_3$), and their polymerization behaviors [8]. Recently we also reported synthesis, structure and catalytic properties of *ansa*-zirconocenes $\text{Me}_2\text{X}(\text{Cp})(\text{RInd})\text{ZrCl}_2$ (X = C, Si; R = 2-*p*- or 3-*p*-tolyl) [9]. As an extension of our studies in this area, we prepared Me_2Si -bridged *ansa*-ligands $\text{Me}_2\text{Si}(\text{RInd})_2$ (R = 2-*p*- (**1**) or 3-*p*-tolyl (**2**)) and their zirconocene complexes $\text{Me}_2\text{Si}(\text{RInd})_2\text{ZrCl}_2$ (R = 2-*p*- (**3**) or 3-*p*-tolyl (**4**)). The two *ansa*-ligands undergo thermal diastereomerization between *rac*- and *meso*-isomers as was observed previously for $\text{Me}_2\text{Si}(\text{Ind})_2$ by Chien [10] and McGlinchey [11]. We herein report details of synthesis of *ansa*-ligands, **1** and **2**, and their thermal diastereomerization in solution. Furthermore, we describe synthesis of *ansa*-zirconocenes, **3** and **4**, and structural characterization of *rac*-**3**, together with the results of propylene polymerization with **3** and **4**/MAO catalyst systems.

2. Results and discussion

2.1. Preparation of **1**–**4**

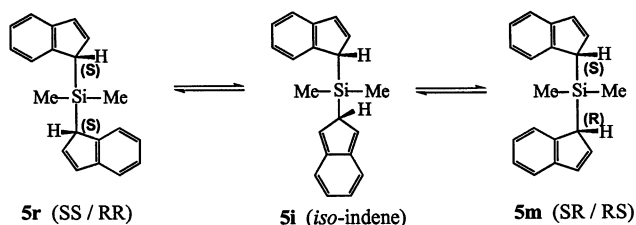
The *p*-tolyl substituted indenenes, 1-*p*-tolylindene and 2-*p*-tolylindene, were prepared by the procedures described in the literature [9]. The *ansa*-ligands, $\text{Me}_2\text{Si}(\text{RInd})_2$ (R = 2-*p*-tolyl (**1**); R = 3-*p*-tolyl (**2**)), could be prepared from the reaction of 2 equiv. of the

lithium salt of the substituted indene with Me_2SiCl_2 . However, use of the corresponding cyanocuprate reagent [12] of the substituted indene results in better yields of a mixture of *rac*- and *meso*-isomers in a ratio of 1:1 for both **1** (83%) and **2** (77%) as shown in Scheme 1. $^1\text{H-NMR}$ spectra of **1** and **2** are consistent with the previous observation that the substitution of Si on indene occurs exclusively at the 1-position of the indene [2,3]. Pure *rac*-isomers, **1r** and **2r**, could be isolated by recrystallization of **1** and **2** in diethyl ether and hexane at -20°C , respectively.

The *ansa*-zirconocenes, **3** (67%, *r:m* = 2:1) and **4** (51%, *r:m* = 1:1), were obtained from the reactions of the dilithio salts of **1** and **2** with zirconium tetrachloride in diethyl ether and hexane at -78°C , respectively. Fractional recrystallization of **3** and **4** in dichloromethane at -20°C gave pure *rac* (**3r**) and *meso* (**4m**) isomers as orange crystals. The $^1\text{H-NMR}$ spectra of **1r**–**4r** (C_2 symmetry) show a single methyl resonance for the two enantiotopic methyl groups on the silicon atom, whereas those of **1m**–**4m** (C_s symmetry) exhibit a pair of singlets for the two diastereotopic methyl groups.

2.2. Diastereomerization of *ansa*-ligands, **1** and **2**

The σ -indenyl derivatives of silicon moiety are well known to be fluxional by migration of either hydrogen atom or silicon moiety [13]. Thermal diastereomerization of *rac*- $\text{Me}_2\text{Si}(\text{Ind})_2$ (**5r**) to *meso*-isomer (**5m**) has been studied, and symmetry-forbidden 1, 3-metalotropic shifts has been proposed as a possible mechanism for the process by Chien and coworkers [10]. McGlinchey and coworkers recently reported that the diastereomerization of **5r** \rightleftharpoons **5m** proceeds by successive symmetry-allowed [1,5]-suprafacial sigmatropic shifts of



Scheme 2.

one $\text{Me}_2\text{Si}(\text{Ind})$ moiety over the surface of the five-membered ring of the other indenyl unit as depicted in Scheme 2 [11]. Furthermore, they isolated the *iso*-indene intermediate which has been trapped as its double Diels-Alder adduct with tetracyanoethylene (TCNE).

The diastereomerization process of $1r \rightleftharpoons 1m$ and $2r \rightleftharpoons 2m$ was studied by $^1\text{H-NMR}$ spectroscopy. $^1\text{H-NMR}$ spectra of $1r$ were recorded in the temperature range from 75 to 95°C in toluene- d_8 . Typical time-resolved $^1\text{H-NMR}$ spectra of $1r$ at 80°C are shown in Fig. 1. As the intensities of the resonances of $1r$ decrease, the resonances corresponding to $1m$ increase in intensity. Relative concentrations of the two diastereomers were measured by integration of the peaks due to the Me_2Si group at $\delta -0.86$ for $1r$ and at $\delta -0.75$ and -0.84 for $1m$. Analyses according to reversible first-order kinetics give excellent fits of experimental data. The kinetic and thermodynamic data are listed in Table 1. The plot of $\ln K_{\text{eq}}$ vs $1/T$ (correlation coefficient, 0.9444) yields $\Delta H_o = 0.67 \pm 0.01 \text{ kcal mol}^{-1}$ and $\Delta S_o = 2.1 \pm 0.8 \text{ cal K}^{-1} \text{ mol}^{-1}$ for the process, $1r \rightarrow$

Table 1
Kinetic and thermodynamic data in toluene- d_8

t (°C)	K_{eq}	$10^3 k_{\text{obs}}$ (min^{-1})	$10^3 k_1$ (min^{-1})	$10^3 k_{-1}$ (min^{-1})
75	1.07 ± 0.01	5.8 ± 0.3	3.0 ± 0.2	2.8 ± 0.1
80	1.10 ± 0.01	12.8 ± 0.6	6.7 ± 0.3	6.1 ± 0.3
85	1.11 ± 0.01	18.2 ± 0.3	9.6 ± 0.2	8.6 ± 0.1
90	1.12 ± 0.01	33.0 ± 2.1	17.5 ± 1.2	15.5 ± 0.9
95	1.13 ± 0.01	54.7 ± 1.4	29.0 ± 0.9	25.7 ± 0.5

$1m$. Activation parameters derived from the Eyring plots of $\ln(k_1/T)$ vs $1/T$ and $\ln(k_{-1}/T)$ vs $1/T$ (correlation coefficients, 0.9807 and 0.9815, respectively) are $\Delta H_1^\ddagger = 25.9 \pm 0.6 \text{ kcal mol}^{-1}$ and $\Delta S_1^\ddagger = 4.4 \pm 2.5 \text{ cal K}^{-1} \text{ mol}^{-1}$ for the forward isomerization $1r \rightarrow 1m$ and $\Delta H_{-1}^\ddagger = 25.2 \pm 0.6 \text{ kcal mol}^{-1}$ and $\Delta S_{-1}^\ddagger = 2.2 \pm 1.3 \text{ cal K}^{-1} \text{ mol}^{-1}$ for the reverse isomerization $1m \rightarrow 1r$. Thermodynamic and kinetic data for 1 and 5 are compared in Table 2. Enthalpy (ΔH_o) of the diastereomerization process for 1 is smaller than that for unsubstituted indenyl compound 5 , whereas activation parameter ΔH_1^\ddagger is larger compared to 5 . These data imply that $1r$ and $1m$ have a similar thermal stability and the 2-*p*-tolyl substituent of the indenyl ligand in 1 has an influence on the diastereomerization process resulting in an increase of the activation energy for the silyl migration. We attempted a Diels-Alder reaction of $1r$ with TCNE, but could not obtain the *iso*-indene intermediate of $1r$.

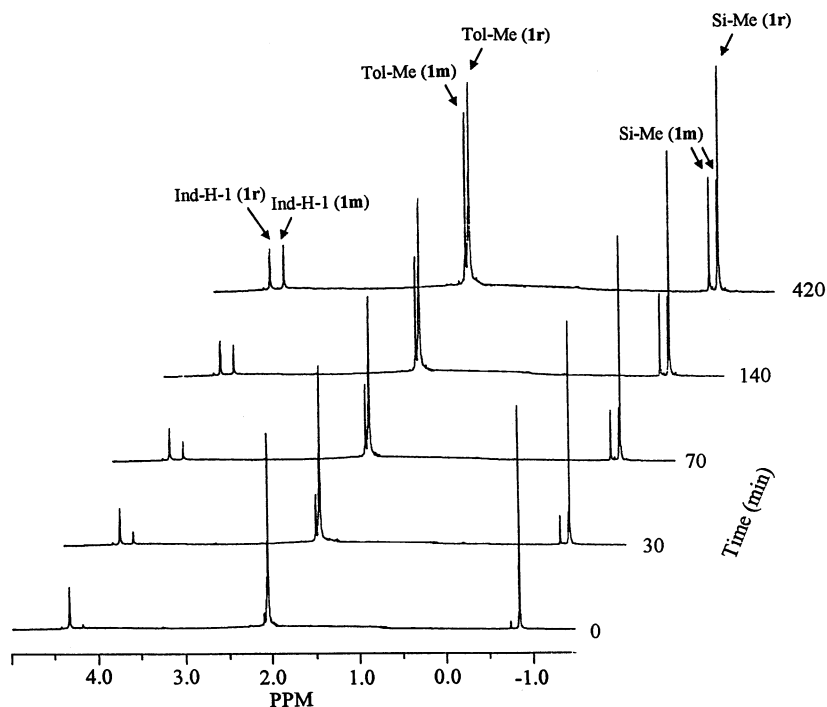


Fig. 1. Time-resolved $^1\text{H-NMR}$ Spectra of $1r$ and $1m$ at 80°C in toluene- d_8 .

Table 2
Comparison of thermodynamic and activation parameters for **1** and **5**

Diastereomerization	ΔH° (kcal mol ⁻¹)	ΔS° (cal mol ⁻¹ K ⁻¹)	ΔH^\ddagger (kcal mol ⁻¹)	ΔS^\ddagger (cal mol ⁻¹ K ⁻¹)	ref.
1r → 1m	0.67 ± 0.01	2.1 ± 0.8	25.9 ± 0.6	4.4 ± 2.5	this work
5r → 5m	7.7	20.7	21.9 ± 0.5	-7.2 ± 1.4	[10,11]

In case of **2r**, no ¹H-NMR spectral change was observed between 75 and 95°C for several hours. After 2 days at 100°C, however, there appeared additional resonances indicating formation of **2m**. The [1,5]-hydrogen shifts has been proposed to explain the formation of 3-silyl isomer of **5**, and is known to occur at elevated temperatures (> 150°C) after prolonged heating [13,14]. It is, therefore, considered that the slow diastereomerization process of **2r** → **2m** at high temperature is due to the hydrogen migration. In order to elucidate the hydrogen migration during the diastereomerization of **2r** ⇌ **2m**, 1,1'-deuterium substituted **2** (**2d**) was prepared by quenching the reaction mixture of **2** and *n*-BuLi with D₂O. The signal at δ 3.72 due to the hydrogen (Ind-H-1) on the carbon-1 of both **2r** and **2m** is absent in the ¹H-NMR spectrum of **2d** (see the bottom spectrum of Fig. 2). When compound **2d** was heated at 110°C for prolonged periods, the signal at δ 3.72 due to Ind-H-1 grows in and the intensity of the two resonances due to the Ind-H-2 of **2r** and **2m** decreases (see Fig. 2). This observation implies that the diastereomerization of **2** occurs by the hydrogen shift as shown in Scheme 3.

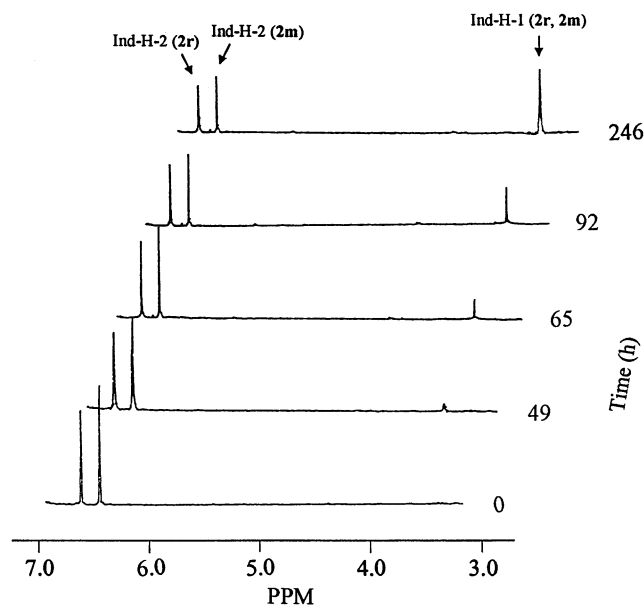


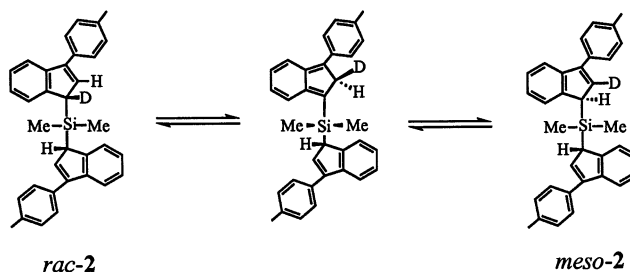
Fig. 2. Time-resolved ¹H-NMR Spectra of **2d** at 110°C in toluene-d₈.

2.3. Crystal structure of **3r** · CHCl₃

The crystal contains an ordered arrangement of discrete Me₂Si(2-TolInd)₂ZrCl₂ · CHCl₃ molecules, which are mutually separated by normal van der Waals distances. The CHCl₃ solvate molecule does not enter into any significant interaction with molecule **3r**. The overall molecular geometry and the atomic labelling scheme of **3r** is illustrated in Fig. 3. Details of the crystallographic data and selected bond distances and angles are shown in Tables 3 and 4, respectively. The overall structure of **3r** is similar to that previously reported for *rac*-Me₂Si(2-MeInd)₂ZrCl₂ [4] and *rac*-Me₂Si(2-Me₂NInd)₂ZrCl₂ [15]. Complex **3r** has a crystallographically imposed C₂ symmetry with Zr and Si atoms on the C₂ axis. Complex **3r** adopts a distorted tetrahedral coordination in which the Ind(Cen)-Zr-Ind(Cen) angle is 127.7 (3)° and the Cl-Zr-Cl bond angle is 94.25 (3)°. The Zr-Cl bond lengths are 2.427 (2) and 2.425 (2) Å. The Zr-Ind (Cen) lengths are 2.229 (7) and 2.246 (7) Å. The Zr-C and Zr-Cl distances as well as Ind(Cen)-Zr-Ind(Cen) and Cl-Zr-Cl angles are comparable to those observed for the two known complexes. The dihedral angle between the two indenyl rings is 62.9 (3)° and those between the indenyl and the *p*-tolyl ring are 48.4 (3) and 57.4 (3)°.

2.4. Propylene polymerization

Polymerization of propylene with complexes **3r** and **4m** in the presence of MAO was carried out in toluene in the temperature range of -30 ~ 50°C. The results are summarized in Table 5 with those of previously known catalyst, *meso*-(1-TolInd)₂ZrCl₂ (**6m**) [8]. The optimum activity for **3r** is observed at 25°C, but the activity decreases drastically at 0°C. Similarly, catalyst system **4m** exhibits a considerable decrease in catalytic activity with decreasing polymerization temperature.



Scheme 3.

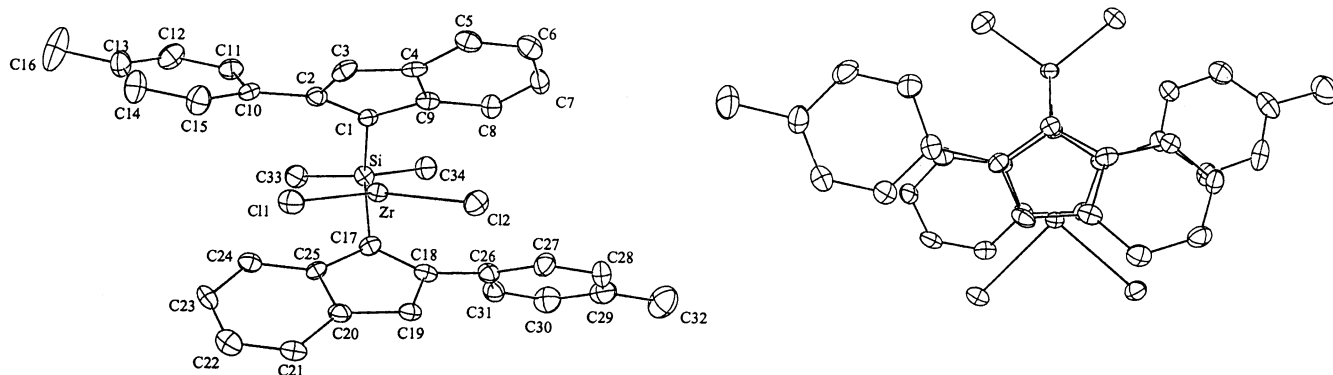


Fig. 3. Molecular structures of **3r** with atomic numbering scheme (left). Projection perpendicular to ZrCl(1)Cl(2) plane (right).

The stereoregularity of PP produced with **3r** and **4m** has been investigated by ^{13}C -NMR spectroscopy. The catalyst **3r** produces isotactic PP with an mm triad intensity of 91% at 0°C . The triad distribution of catalyst **3r** follows the enantiomorphic site control propagation statistics ($2(\text{rr})/(\text{mr}) = 1.0$), indicating that the isotactic portion of the polymer was controlled by the chirality of catalyst [16]. As shown in Fig. 3, the *p*-tolyl group in **3r** is oriented toward the lateral sector of the bent metallocene wedge, which consequently has little influence on enantiofacial coordination of the incoming propylene monomer to produce iPP.

We previously described that the unbridged metallocene **6m** affords PP at -30°C having dominantly a

syndiotactic stereosequence (see Table 5). Complex **4m**, a bridged analogue of **6m**, also affords a syndiotactic dominant PP. The ^{13}C -NMR spectrum of the PP with **4m** is consistent with the Bernoullian propagation statistics ($4(\text{mm})(\text{rr})/(\text{mr})^2 = 1.0$) for the chain end controlled stereospecific polymerization [16]. The catalyst **6m** has shown complete loss of the syndiotacticity of the polymer with increasing polymerization temperature, whereas the syndiotacticity of PP with catalyst **4m** remains comparable in the temperature range of $-30 \sim 25^\circ\text{C}$. This result indicates that the presence of a bridging group renders the rigidity of π -ligands to catalysts, producing a stereospecific polymer without a significant temperature effect.

Table 3
Crystallographic data for complex **3r** · CHCl₃

Formula	C ₃₅ H ₃₀ Cl ₅ SiZr
f_w	748.2
Crystal system	Triclinic
Space group	<i>P</i> -1
<i>a</i> (Å)	12.912 (2)
<i>b</i> (Å)	15.773 (4)
<i>c</i> (Å)	9.280 (1)
α (°)	99.18 (2)
β (°)	99.95 (1)
γ (°)	113.75 (2)
<i>V</i> (Å ³)	1647.9 (5)
<i>Z</i>	2
D_{calcd} (g cm ⁻³)	1.508
Temp (K)	298
Crystal size (mm)	0.07 × 0.5 × 0.3
Radiation	Graphite-monochromated Mo-K α
μ (mm ⁻¹)	0.80
scan mode	$\omega/2\theta$
$2\theta_{\text{max}}$ (°)	47.8
No. of unique reflns	5156
No. of reflns ($I > 3\sigma(I)$)	2820
No. of params	499
R^a	0.045
R_w^b	0.051
GOF	0.58

^a $R = \sum ||F_o| - |F_c|| / \sum |F_o|$

^b $R_w = [\sum (|F_o| - |F_c|)^2 / \sum |F_o|^2]^{1/2}$

^c $\text{GOF} = [\sum (|F_o| - |F_c|)^2 / (\text{No. of reflns} - \text{No. of params})]^{1/2}$

3. Experimental section

3.1. General comments

All reactions were carried out under an inert atmosphere of argon by using either standard Schlenk or glovebox techniques. Tetrahydrofuran (THF), diethyl ether, hexane and toluene were distilled from sodium-

Table 4
Selected bond distances and bond angles for **3r** with estimated standard deviations

Bond distances (Å)			
Zr–Cl(1)	2.427(2)	Zr–C(18)	2.554(8)
Zr–Cl(2)	2.425(2)	Zr–C(19)	2.598(8)
Zr–C(1)	2.472(7)	Zr–C(20)	2.623(8)
Zr–C(2)	2.553(8)	Zr–C(25)	2.512(8)
Zr–C(3)	2.554(8)	Si–C(1)	1.887(8)
Zr–C(4)	2.604(8)	Si–C(17)	1.889(8)
Zr–C(9)	2.507(8)	Zr–Ind(Cen) ^a	2.229(7)
Zr–C(17)	2.481(7)	Zr–Ind(Cen)	2.246(7)
Bond angles (°)			
Cl(1)–Zr–Cl(2)	94.2 (3)	Ind(Cen)–Zr–Ind(Cen)	127.7(3)
C(1)–Si–C(17)	94.5(3)	Ind–Ind ^b	62.9(3)
C(33)–Si–C(34)	105.7(5)		

^a Cen = ring centroid.

^b Interplanar angle between the two indenyl ligands.

Table 5
 Polymerization^a of propylene with **3r** and **4m**/MAO catalyst systems

Metalloenes	Zr (μmol)	MAO (mmol)	T_p ($^{\circ}\text{C}$)	t_p (h)	Yield (g)	A^b	\bar{M}_w ($\times 10^{-3}$)	MWD	mm	mr	rr	Ref.
3r	15	15	50	1.2	4.00	190.5			0.37	0.38	0.25	This work
	15	15	25	1	6.90	383.3	1.3	1.72	0.70	0.20	0.10	
	15	30	0	1	1.06	59.0	4.4	1.68	0.91	0.07	0.02	
4m	20	40	25	5	15.15	126.3			0.15	0.45	0.40	This work
	20	40	0	5	7.40	61.7	3.6	2.22	0.08	0.48	0.44	
	20	40	-30	5	0.84	7.0	15.1	2.17	0.11	0.44	0.45	
6m	8	40	25	2	2.84	147.9			0.30	0.47	0.23	[8]
	16	40	-30	6	12.00	104.2	37.8	2.52	0.09	0.42	0.49	

^a Polymerization conditions: 1.2 atm, toluene (250 ml).

^b Activity in (kg of PP)/(mol of Zr) [monomer] h).

benzophenone under N_2 atmosphere. Dichloromethane was refluxed over CaH_2 and then distilled under N_2 atmosphere. Silica gel (Merck, 230-400 mesh) was used for column chromatography. 1-*p*-Tolyindene and 2-*p*-tolyindene were prepared by the procedures reported previously [9]. The ^1H -NMR and ^{13}C -NMR spectra were obtained on a Bruker AC-200 or AM-300 FT-NMR spectrometer. Mass spectra were recorded on a JEOL SX 102 spectrometer. All m/z values are referenced to ^{28}Si and ^{35}Cl . Microanalytical data were provided by the Analytical Laboratory of the Korea Basic Science Institute Seoul Branch.

Molecular masses were determined by gel permeation chromatography on a Waters 150CV⁺ instrument in 1,2,4-trichlorobenzene at 135°C . The ^{13}C -NMR (75 MHz) spectra of the resulting polymers were recorded at 100°C on a Bruker AMX-300 FT-NMR spectrometer. The polymer samples were dissolved in 1,2,4-trichlorobenzene/benzene- d_6 (4/1 by vol.) up to a concentration of 15 wt.% at 130°C in NMR tubes (10 mm o.d.).

3.2. Preparation of bis(2-*p*-tolyindenyl)dimethylsilane (**1**)

A 500 ml Schlenk flask was charged with 2-*p*-tolyindene (0.75 g, 3.6 mmol), copper cyanide (0.01 g, 0.11 mmol), and diethyl ether (30 ml). To the mixture was added dropwise a solution of *n*-butyllithium (1.6 M, 2.5 ml, 4.00 mmol) at -20°C . After the addition was complete, the reaction mixture was allowed to warm up to room temperature for 2 h. Then a solution of dimethyldichlorosilane (0.24 ml, 2.00 mmol) in THF (10 ml) was added dropwise at room temperature. The resulting mixture was stirred overnight and treated with a saturated solution of NH_4Cl in water (100 ml). The solution was extracted with diethyl ether and dried over anhydrous magnesium sulfate. The crude product was purified with

preparative TLC (hexane) to afford **1** (0.71 g, 1.5 mmol, 83%) as a pale yellow powder (*r/m* ratio, 1:1). Fractional recrystallization from diethyl ether at -20°C afforded pure **1r** (0.30 g, 0.64 mmol, 35%) as a colorless powder. Isomer **1m** was obtained from the filtrate as a pale yellow oil after removal of the solvent. Compound **1r**: ^1H -NMR (CDCl_3 , 25°C) δ 7.56–7.02 (18H, m, C_6 indenyl and tolyl), 4.42 (2H, H-C(1)), 2.30 (6H, s, tolyl CH_3), -0.94 (6H, s, $\text{Si}(\text{CH}_3)_2$). MS (70 eV): m/z 468 (M^+). Anal. Calcd for $\text{C}_{34}\text{H}_{32}\text{Si}$: C, 87.13; H, 6.88. Found: C, 87.37; H, 8.17. Compound **1m**: ^1H -NMR (CDCl_3 , 25°C): δ 7.55–7.01 (18H, m, C_6 indenyl and tolyl), 4.22 (2H, H-C(1)), 2.33 (6H, s, tolyl CH_3), -0.81 (3H, s, $\text{Si}(\text{CH}_3)_2$), -1.02 (3H, s, $\text{Si}(\text{CH}_3)_2$).

3.3. Preparation of bis(3-*p*-tolyindenyl)dimethylsilane (**2**)

1-*p*-Tolyindene (1.85 g, 9.0 mmol), copper cyanide (0.024 g, 0.3 mmol), *n*-butyllithium (1.6 M, 6.2 ml, 10.0 mmol) and dichlorodimethylsilane (0.58 g, 4.5 mmol) were treated by a procedure similar to that for the preparation of **1**, producing **2** (1.61 g, 3.4 mmol, 77%) as an orange oil (*r/m* ratio, 1:1). Fractional recrystallization of **2** from hexane at -20°C afforded pure **2r** (0.63 g, 1.3 mmol, 30%) as a colorless powder. Isomer **2m** was collected from the filtrate as an orange oil after evaporation of the solvent. Compound **2r**: ^1H -NMR (CDCl_3 , 25°C) δ 7.66–7.23 (16H, m, C_6 indenyl and tolyl), 6.63 (2H, d, $J=2.1$ Hz, H-C(2)), 3.72 (2H, d, $J=2.1$ Hz, H-C(1)), 2.41 (6H, s, tolyl CH_3), -0.21 (6H, s, $\text{Si}(\text{CH}_3)_2$). MS (70 eV): m/z 468 (M^+). Anal. Calcd for $\text{C}_{34}\text{H}_{32}\text{Si}$: C, 87.13; H, 6.88. Found: C, 88.48; H, 8.52. Compound **2m**: ^1H -NMR (CDCl_3 , 25°C): δ 7.56–7.19 (16H, m, C_6 indenyl and tolyl), 6.41 (2H, d, $J=2.1$ Hz, H-C(2)), 3.72 (2H, d, $J=2.1$ Hz, H-C(1)), 2.39 (6H, s, tolyl CH_3), -0.20 (3H, s, $\text{Si}(\text{CH}_3)_2$), -0.40 (3H, s, $\text{Si}(\text{CH}_3)_2$).

3.4. Preparation of bis(3-*p*-tolylindenyl)dimethylsilane-1,1'-*d*₂ (**2d**)

To a solution of **2** (0.9 g, 1.9 mmol) in diethyl ether (30 ml) was added *n*-butyllithium (1.47 M, 2.7 ml, 3.9 mmol) in hexane at -78°C . The reaction mixture was allowed to warm up to room temperature for 3 h, treated with D₂O (0.7 ml, 38.4 mmol), and dried over anhydrous magnesium sulfate. The resulting suspension was filtered and the filtrate was evaporated in vacuo. The crude product was purified with preparative TLC (hexane) to give **2d** (0.72 g, 1.5 mmol, 80%) as an orange oil. ¹H-NMR (CDCl₃, 25°C): δ 7.67–7.24 (16H, m, C₆ indenyl and tolyl), 6.63 (1H, s, H–C(3)), 6.43 (1H, s, H–C(3)), 2.42 (3H, s, tolyl CH₃), 2.41 (3H, s, tolyl CH₃), 0.08 (3H, s, Si(CH₃)₂), -0.21 (3H, s, Si(CH₃)₂), -0.41 (3H, s, Si(CH₃)₂) for an isomeric mixture. MS (70 eV): m/z 470 (M⁺).

3.5. ¹H-NMR study of diastereomerization of **1r** to **1m**

A colorless powder of compound **1r** (ca. 5 mg) was transferred to five 5-mm NMR tubes and toluene-*d*₈ (0.5 ml) was added to each NMR tube under the atmosphere of nitrogen. The tubes were sealed, then heated in an NMR probe at 75, 80, 85, 90, and 95°C, and monitored periodically by ¹H-NMR spectroscopy.

3.6. Preparation of dimethylsilanediylbis(2-*p*-tolylindenyl)zirconium dichloride (**3**)

A solution of *n*-butyllithium (1.36 M, 2.5 ml, 3.4 mmol) in hexane was added to a solution (40 ml) of **1** (0.76 g, 1.6 mmol) in diethyl ether and hexane at -78°C . During warming to room temperature for 2 h the reaction mixture changed from a red-orange to a pink suspension. The pink suspension was added to a suspension of zirconium tetrachloride (0.46 g, 1.99 mmol) in diethyl ether (10 ml) and hexane (10 ml) at -78°C . Immediately after the addition the cooling bath was removed. The suspension was stirred overnight. The orange precipitate formed was filtered and washed three times with diethyl ether (3 × 10 ml). The orange solid was extracted with dichloromethane (20 ml) and the extract was evaporated to give red-orange compound **3** (0.69 g, 1.1 mmol, 67%) as a 2:1 mixture of the *rac*- and *meso*-isomers. Fractional crystallization from dichloromethane at -20°C afforded pure **3r** (0.39 g, 0.62 mmol, 38%). Compound **3r**: ¹H-NMR (CDCl₃, 25°C): δ 7.58–6.66 (18H, m, indenyl and tolyl), 2.40 (6H, s, tolyl CH₃), 0.87 (6H, s, Si(CH₃)₂). MS (70 eV): m/z 628 (M⁺). Compound **3m** (data obtained from an isomeric mixture): ¹H-NMR (CDCl₃, 25°C): δ 7.73–6.84 (18H, m, indenyl and tolyl), 2.23 (6H, s, tolyl CH₃), 1.51 (3H, s, Si(CH₃)₂), 0.51 (3H, s, Si(CH₃)₂).

3.7. Preparation of dimethylsilanediylbis(3-*p*-tolylindenyl)zirconium dichloride (**4**)

Compound **2** (1.61 g, 3.43 mmol), *n*-butyllithium (1.27 M, 5.54 ml, 7.03 mmol), and zirconium tetrachloride (0.80 g, 3.43 mmol) were treated as described for the preparation of **3**, providing orange compound **4** (1.00 g, 1.6 mmol, 51%) as a 1:1 mixture of the *rac*- and *meso*-isomers. Fractional crystallization from dichloromethane at -20°C produced pure **4m** (0.39 g, 0.62 mmol, 20%). Compound **4m**: ¹H-NMR (CDCl₃, 25°C): 7.78–6.92 (16H, m, indenyl and tolyl), 5.96 (2H, s, C₅ indenyl) 2.30 (6H, s, tolyl CH₃), 1.43 (3H, s, Si(CH₃)₂), 0.94 (3H, s, Si(CH₃)₂). MS (70 eV): m/z 628 (M⁺). Compound **4r** (data obtained from an isomeric mixture): ¹H-NMR (CDCl₃, 25°C): δ 7.80–7.00 (16H, m, indenyl and tolyl), 6.14 (2H, s, C₅ indenyl) 2.32 (6H, s, tolyl CH₃), 1.16 (6H, s, Si(CH₃)₂).

3.8. X-ray data collection and structure solution of **3r** · CHCl₃

Crystals of **3r** suitable for an X-ray analysis were obtained by slow crystallization from chloroform at -20°C . An orange crystal of the appropriate dimensions was sealed under N₂ in a thin walled glass capillary. Preliminary examination and data collection were performed using an Enraf-Nonius CAD4 diffractometer equipped with a graphite monochromated Mo–K_α radiation at 298 K. Relevant crystallographic data are summarized in Table 2. Orientation matrices and unit cell parameters were determined by least-square method of 25 reflections with $22.76 < \theta < 28.06^{\circ}$. Intensity data for 5165 independent reflections in the range $-14 \leq h \leq 13$, $0 \leq k \leq 18$, $-10 \leq l \leq 10$ were collected using $\omega/2\theta$ scan mode, ω scan angle = $(0.8 + 0.35 \tan \theta)^{\circ}$, $2\theta_{\text{max}} = 45^{\circ}$. Three standard reflections were monitored every 3 h, which revealed no significant decay over the course of data collection. Lorentz and polarization corrections were applied to the intensity data. All the calculations were carried out using the NRCVAX software package [17]. The structure was solved by direct and different Fourier methods and refined by the full matrix least-squares methods employing unit weights. All nonhydrogen atoms were refined anisotropically, while hydrogen atoms were refined isotropically. Final reliability factors for 2820 unique observed reflections [$F_o > 3\sigma(F_o)$] were $R_f = 0.045$ and $R_w = 0.051$. The large shift/esd was 0.269, and the maximum and minimum hole in the final difference map were 0.85 and $-0.44 \text{ e}^{\text{Å}}^{-3}$. Atomic coordinates for the non-hydrogen atoms are listed in Table 6.

3.9. Polymerization procedure

Solution polymerization reactions in toluene were

Table 6
Atomic coordinates and equivalent isotropic displacement coefficients ($\text{\AA}^2 \times 10^2$) for $3r \cdot \text{CHCl}_3$

Atom	x	y	z	U_{eq}^a
Zr	0.2781(1)	0.7932(1)	0.0759(1)	2.05(4)
Cl(1)	0.3506(2)	0.7354(2)	-0.1239(2)	2.9(1)
Cl(2)	0.2597(2)	0.9177(2)	-0.0337(2)	3.1(1)
Si	0.2207(2)	0.7232(2)	0.3854(2)	2.2(1)
C(1)	0.3575(6)	0.8104(5)	0.3467(8)	2.1(4)
C(2)	0.4387(7)	0.7903(6)	0.2760(9)	2.4(4)
C(3)	0.4954(7)	0.8672(7)	0.2143(9)	2.7(5)
C(4)	0.4631(6)	0.9404(6)	0.2546(8)	2.4(4)
C(5)	0.5022(7)	1.0347(6)	0.233(1)	3.0(5)
C(6)	0.4545(8)	1.0888(7)	0.291(1)	3.1(5)
C(7)	0.3650(8)	1.0547(6)	0.363(1)	3.0(5)
C(8)	0.3241(8)	0.9661(6)	0.3854(9)	2.8(4)
C(9)	0.3738(7)	0.9050(6)	0.3350(8)	2.5(4)
C(10)	0.4738(7)	0.7134(6)	0.2802(9)	2.8(4)
C(11)	0.4972(8)	0.6867(7)	0.415(1)	3.3(5)
C(12)	0.5453(8)	0.6249(7)	0.427(1)	3.9(6)
C(13)	0.5754(8)	0.5853(7)	0.305(1)	3.7(5)
C(14)	0.552(1)	0.6109(8)	0.173(1)	4.4(6)
C(15)	0.5043(9)	0.6734(7)	0.160(1)	3.9(6)
C(16)	0.628(2)	0.518(1)	0.322(3)	7.0(1)
C(17)	0.1274(7)	0.6894(6)	0.1856(8)	2.4(4)
C(18)	0.0730(7)	0.7410(6)	0.1163(8)	2.5(4)
C(19)	0.0529(7)	0.7141(6)	-0.0409(9)	2.4(4)
C(20)	0.0869(7)	0.6394(6)	-0.0785(9)	2.7(4)
C(21)	0.0764(7)	0.5805(6)	-0.2199(9)	2.8(4)
C(22)	0.1131(8)	0.5130(7)	-0.218(1)	3.2(5)
C(23)	0.1645(8)	0.4994(6)	-0.0810(9)	2.8(4)
C(24)	0.1783(7)	0.5545(6)	0.0550(9)	2.8(4)
C(25)	0.1353(6)	0.6252(6)	0.0616(8)	2.1(4)
C(26)	0.0243(7)	0.8018(6)	0.1879(9)	2.7(4)
C(27)	0.0379(8)	0.8877(7)	0.157(1)	3.2(5)
C(28)	-0.023(1)	0.9345(8)	0.212(1)	4.5(6)
C(29)	-0.1019(9)	0.8987(8)	0.295(1)	4.2(6)
C(30)	-0.115(1)	0.8112(9)	0.327(1)	4.3(6)
C(31)	-0.1538(8)	0.7659(7)	0.273(1)	3.1(5)
C(32)	-0.167(2)	0.953(1)	0.346(2)	6.0(1)
C(33)	0.227(1)	0.6190(9)	0.446(1)	3.6(6)
C(34)	0.171(1)	0.7807(8)	0.531(1)	3.2(6)

^a U_{eq} is defined as one-third of the trace of the orthogonalized U_{ij} tensor.

carried out at a propylene pressure of 1.2 atm, agitating with a Teflon magnetic spinbar in a 500 ml glass reactor. Toluene (200 ml) was introduced into the reactor, temperature was increased to the polymerization temperature, and then toluene was saturated with propylene. A toluene solution of the Zr catalyst and MAO purchased from Toso-Akzo as a toluene solution was injected into the reactor by a tuberculin syringe, and polymerization was started. Propylene concentrations in the liquid phase was calculated with a com-

puter program for the gas–liquid phase equilibria based on Chao-Sender correlations. After polymerization was terminated by injecting ethanol, the resulting polymer was quenched with an excess of acidified methanol (ca. five times of the amount of toluene used). The precipitated polymer was separated from the polymerization medium by cooling to -30°C , washed with fresh ethanol, and dried in vacuo.

Acknowledgements

We are grateful to the Korea Academy of Industrial Technology for the financial support of this work.

References

- [1] (a) J.A. Ewen, *J. Am. Chem. Soc.* 106 (1984) 635. (b) W. Kaminsky, K. Külper, H.H. Brintzinger, F.R.W.P. Wild, *Angew. Chem. Int. Edn. Engl.* 24 (1985) 507. (c) J.A. Ewen, L. Haspeslagh, J.L. Atwood, H. Zhang, *J. Am. Chem. Soc.* 109 (1987) 6544. (d) W. Röhl, H.H. Brintzinger, B. Rieger, R. Zolk, *Angew. Chem. Int. Edn. Engl.* 29 (1990) 279.
- [2] W. Spaleck, F. Küber, A. Winter, J. Röhrmann, B. Bachmann, M. Antberk, E.F. Paulus, *Organometallics* 13 (1994) 945.
- [3] U. Stehling, J. Diebold, W. Röhl, H.H. Brintzinger, S. Jungling, R. Mülhaupt, F. Langhauser, *Organometallics* 13 (1994) 964.
- [4] W. Spaleck, M. Antberk, J. Röhrmann, A. Winter, B. Bachmann, P. Kiprof, J. Behm, W.A. Hermann, *Angew. Chem. Int. Edn. Engl.* 31 (1992) 1347.
- [5] (a) J.A. Ewen, J.L. Jones, A. Razavi, J.D. Ferrara, *J. Am. Chem. Soc.* 110 (1988) 6255. (b) A. Razavi, J. Ferrara, *J. Organomet. Chem.* 435 (1992) 299. (c) A. Razavi, J.L. Atwood, *J. Organomet. Chem.* 459 (1993) 117.
- [6] (a) G. Erker, B. Tomme, *J. Am. Chem. Soc.* 114 (1992) 4004. (b) G. Erker, M. Albach, M. Knickmeier, D. Wingbermahle, C. Krüger, M. Nolte, S. Werner, *J. Am. Chem. Soc.* 115 (1993) 4590. (c) E. Hauptman, R.M. Waymouth, *J. Am. Chem. Soc.* 117 (1995) 11586.
- [7] G.W. Coates, R.M. Waymouth, *Science* 267 (1995) 217.
- [8] T.K. Han, S.C. Yoon, Y.S. Ko, B.W. Woo, J.T. Park, S.I. Woo, *Polymer Bull.* 37 (1996) 35.
- [9] S.C. Yoon, T.K. Han, B.W. Woo, H. Song, S.I. Woo, J.T. Park, *J. Organomet. Chem.* 534 (1997) 81.
- [10] Y.-X. Chen, M.D. Rausch, J.C.W. Chien, *Organometallics* 12 (1993) 4607.
- [11] S.S. Rigby, L. Girard, A.D. Bain, M.J. McGlinchey, *Organometallics* 14 (1995) 3798.
- [12] P. Kocienski, S. Wadman, *J. Am. Chem. Soc.* 111 (1989) 2363.
- [13] P. Jutzi, *Chem. Rev.* 86 (1986) 983.
- [14] R.B. Larrabee, B.F. Dowden, *Tetrahedron Lett.* 12 (1970) 915.
- [15] E. Barsties, S. Schaible, M.-H. Prosenc, U. Rief, W. Roll, O. Weyand, B. Dorrer, H.-H. Brintzinger, *J. Organomet. Chem.* 520 (1996) 63.
- [16] J.A. Ewen, *J. Am. Chem. Soc.* 106 (1984) 4226.
- [17] E.J. Gabe, Y.L. Page, J.P. Charland, F.L. Lee, P.S. White, *J. Appl. Cryst.* 22 (1989) 384.